Lanthanum phosphate as catalyst in the reaction of 5-HMF formation

Ika F. Ulfindrayani[1], *Agustino* Zulys[2], *Fredy* Kurniawan[1], *Qurrota* A'yuni[3], *Hilfi* Pardi[4], and *Irmina* K. Murwani[1]

[1]Institut Teknologi Sepuluh Nopember, Department of Chemistry, Surabaya, Jawa Timur, Indonesia, 60111

[2]Universitas Indonesia, Department of Chemistry, Depok, Jawa Barat, Indonesia, 16424

[3]Universitas Airlangga, Department of Chemistry, Surabaya, Jawa Timur, Indonesia, 60115

[4]Universitas Maritim Raja Ali Haji, Department of Chemistry Education, Tanjungpinang, Kepulauan Riau, Indonesia, 29111

Abstract. Lanthanum phosphate (LP) has been synthesized by sol-gel method at room temperature. The synthesized catalyst was characterized by X-ray diffraction (XRD), Fourier Transform Infrared (FTIR), pyridine adsorption FTIR, N_2 adsorption-desorption and SEM-EDX. The XRD results show that LP has a hexagonal structure. The FTIR spectra of LP showed O=P-O bending vibrations, P-O vibrations (from phosphate tetrahedral distortion), P-O symmetrical strain vibrations and PO_4^{3-} bending vibrations, each of which was characterized by the appearance of a peak at 613, 530-620, 950 and 538-621 cm^{-1}. The presence of the OH functional group was indicated by a peak at 3450-3700 cm^{-1}, which was strengthened by the H-O-H bending vibration that appeared at 1629 cm^{-1}. The surface area, pore volume and pore diameter of LP are 51.04 m^2/g, 0.21 cm^3/g and 13.31 nm, respectively. SEM image showed that agglomerated solids with irregular shapes were obtained from the synthesis. Catalytic testing indicates that the acidity of the catalyst has main role in the formation of 5-HMF.

1 Introduction

Rare earth elements are elements that are very rare or in tiny amounts. Rare earth elements have been discovered in nature as complex compounds, which are generally complex compounds of phosphate and carbonate. There are two types of minerals that contain rare earth elements, namely monazite and xenotim minerals. Examples of monazite minerals are $CePO_4$, $NdPO_4$, YPO_4, $LaPO_4$, and others [1]. Lanthanum phosphate or often called lanthanum orthophosphate ($LaPO_4$) has drawn the great attention of many researchers due to its many potencies, especially for application optics as phosphorus [2]. Lanthanum phosphate ($LaPO_4$) has excellent properties and various applications, including catalyst [3], hydrophobic nano-coating [4], bio-imaging, bio-labeling [5], and photoluminescence material [6].

$LaPO_4$ catalyst has two types of acid at a time that is Bronsted acid from group hydroxyl on the phosphate ion and Lewis's acid derived from central metal ions, the acid site present in the framework structure metal phosphate is flexible, as well as a simple synthesis process [7]. $LaPO_4$ catalyst can be used in dehydration catalysts [8]. The synthesis of $LaPO_4$ was carried out using various methods for catalysts in the 1-butanol dehydration reaction where the results obtained showed that the catalyst activity was very dependent on the Brønsted acid nature of the $LaPO_4$ phosphate group. A catalytic reaction with $LaPO_4$ has yet to be carried out for cellulose conversion to 5-hydroxymethylfurfural (5-HMF). 5-HMF is produced by dehydrating fructose and glucose, as well as by hydrolyzing cellulose [9].

5-HMF is an intermediate compound resulting from the conversion of cellulose and dehydration of hexose [10]. 5-HMF has been listed among the top ten value-added chemicals derived from biomass by the United States Department of Energy [11]. 5-HMF is an essential platform chemical in biorefineries. 5-HMF is a precursor compound for the synthesis of a series of valuable chemicals into liquid fuels such as 2,5-furan dicarboxylic acid (FDCA), 2,5-dimethyl furan (DMF) and Levulinic acid (LA) [12]. Therefore, in this research, LP catalyst synthesis was carried out using the sol gel method. The resulting LP catalyst will be tested for its catalytic activity in the reaction to form 5-HMF from cellulose, glucose and fructose.

2 Experimental

2.1 Materials

$LaCl_3.7H_2O$ (98%, Merck), H_3PO_4 (99%, Merck), NH_4OH (25%, Merck), 5-hydroxumethylfurfural, cellulose, glucose, fructose, distilled water and aquabidest (Otsuka) were used without additional purification.

2.2 Catalyst Preparation

The synthesized of LP via sol-gel method by reacting the solution of $LaCl_3 \cdot 7H_2O$ and H_3PO_4. NH_4OH solution was added to adjust the pH level and the resulting gel was aged until it became stable. Afterward, the gel was decanted and dried at 100℃ to remove the solvent. Finally, the dried gel calcined at 550℃ for 4 hours to obtained LP powder.

2.3 Catalyst Characterization

The XRD analysis was performed using Cu Kα (1.54056Å) radiation in the 2θ range of 20-90° with a 0,05° interval on a Philips X-Pert instrument.

The chemical bonds of the powder was determined using FTIR Shimadzu Instrument Spectrum One 8400s.

The acidity of powder was determined using FTIR-pyridine adsorption method [14]. The powder were poured with 30 µL of pyridine. After that, it was heated for 3 hours at 150℃ under N_2 conditions. The FTIR spectra of pyridine adsorbed samples were recorded and analyzed at wave numbers 1400-1750 cm^{-1} after cooling.

The S_{BET} surface area of the powder was measured by Quantachrome Nova instrument using N_2 adsorption-desorption isotherm method at -196℃. The samples were degassed with nitrogen at a flow rate of 30 cm^3/minute at 150℃ for 3 hours.

The morphology of the powder was observed by SEM-EDX on Hitachi Flexem 100 instrument.

2.4 Catalytic Test

The performance of the synthesized catalyst was tested through the production of 5-HMF from cellulose, glucose, and fructose conversion reaction. The initial reactant (0.15 g) was reacted with 50 mL of 0.03% HCl solution in a reflux system at a temperature of 100℃ for 30 minutes. The mixture is put into teflon and added to the catalyst used. Next, the teflon is put into an autoclave and heated in an oven at 220℃ for 150 minutes. After the reaction process, the catalyst and remaining reactants are separated from the filtrate by a filtering process. The filtrate was analyzed for the presence of 5-HMF using UV-Vis spectrophotometer.

3 Result and Discussion

3.1 Catalytic Characterization

XRD diffractogram of LP was shown in Fig. 1. The XRD pattern was matched with JCPDS-International Centre of Diffraction Data PCPDFWIN. The matching results show that the diffractogram of the synthesized catalyst matches the three main peaks of the standard $LaPO_4$ diffractogram (PDF No. 04-0635) at 2θ = 28.69 (200); 31.16 (102) and 41.58° (211) which indicates the formation of $LaPO_4$ which has a hexagonal structure [13]. This is following research conducted by Ahmadzadeh *et al.*, (2019) [14], namely the synthesized $LaPO_4$ solid with peaks at 2θ = 29, 31, and 41°. In the diffractogram it can be seen that the peak at 29° (200) shows a higher intensity than the peak at 31° (102) which indicates crystal growth in the hexagonal plane of the c axis [15,16].

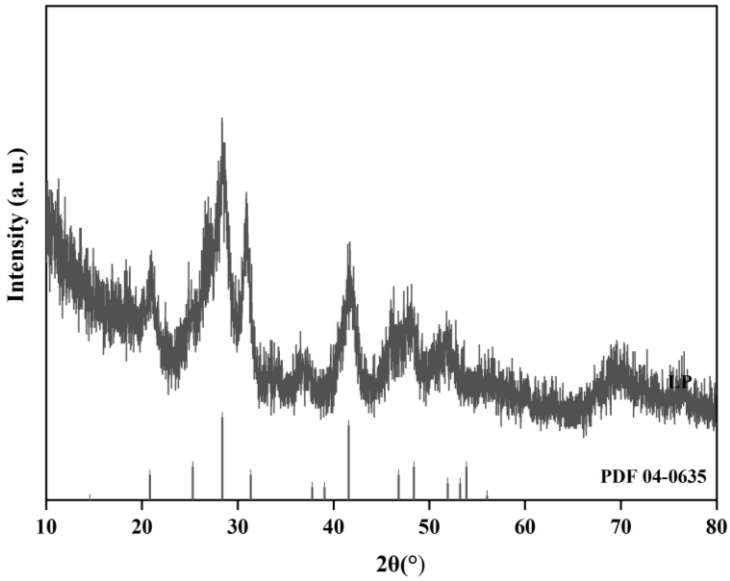

Fig. 1. XRD pattern of LP

Characterization with FTIR was carried out at wavenumber 400-4000 cm^{-1}. The FTIR spectra of LP is shown in Fig. 2. In the picture seen that the vibration observed at 3450-3700 cm^{-1}, shows the existence of vibration stretch OH on the H_2O molecule. This is supported by the existence peak at 1629 cm^{-1} which shows the existence of H_2O vibration. That peak experiences the shift caused by the interaction OH group on the surface. The absorption bands at 540 and 613 cm^{-1} are associated with the vibration bend O-P-O and bending vibration O=P-O. This is the same as the research conducted by Wang et al. [17] where in the wavenumber 530-620 cm^{-1} is a deformation band asymmetrical P-O and reinforced study Niu et al. [18] where vibration PO_4^{3-} at 538-621 cm^{-1}. There is a symmetrical stretching vibration P-O on the wavenumber 950 cm^{-1} and asymmetric stretching vibration O=P-O on the wavenumber 1047 cm^{-1}.

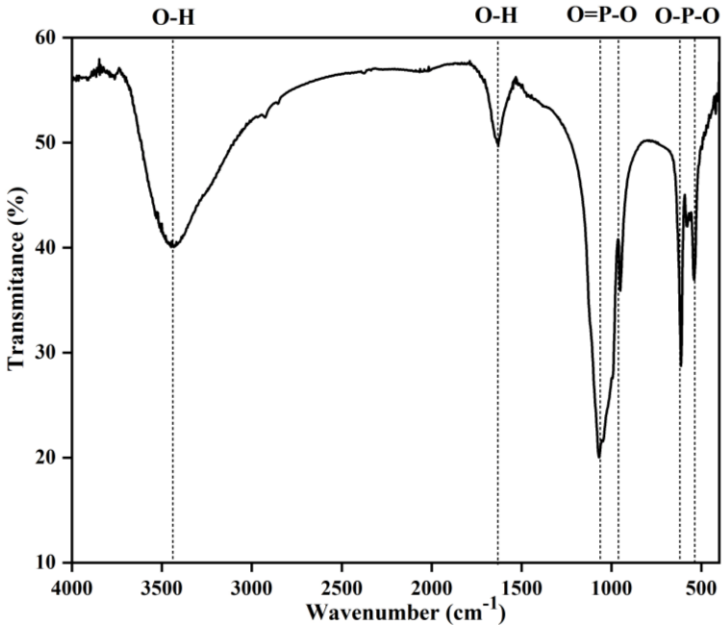

Fig. 2. FTIR spectra of LP

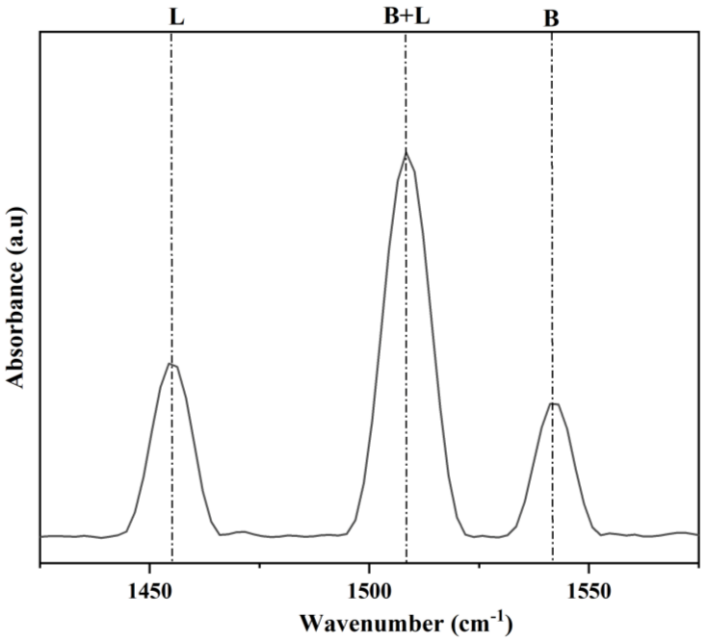

Fig. 3. FTIR pyridine spectra of LP

The surface acid sites of samples were determined from FTIR spectra of adsorbed pyridine samples, the results were shown in Fig. 3 indicated that there are three types of acid on the catalyst surface, namely Lewis acid (L), combination of Lewis and Brønsted acid (B+L) and Brønsted acid (B). The Lewis acid side of the LP catalysts appears at 1454 cm^{-1}. This is in accordance with Layman et al., 2003 which states that the Lewis acid side appears in the region 1445-1464 cm^{-1} [19]. The Brønsted acid side is shown in the region of 1540 cm^{-1} [20,21]. In this study, the Brønsted acid side found in all catalysts appeared at 1541 cm^{-1}. The combination of Lewis acid and Brønsted acid sites appears at 1508 cm^{-1} [22].

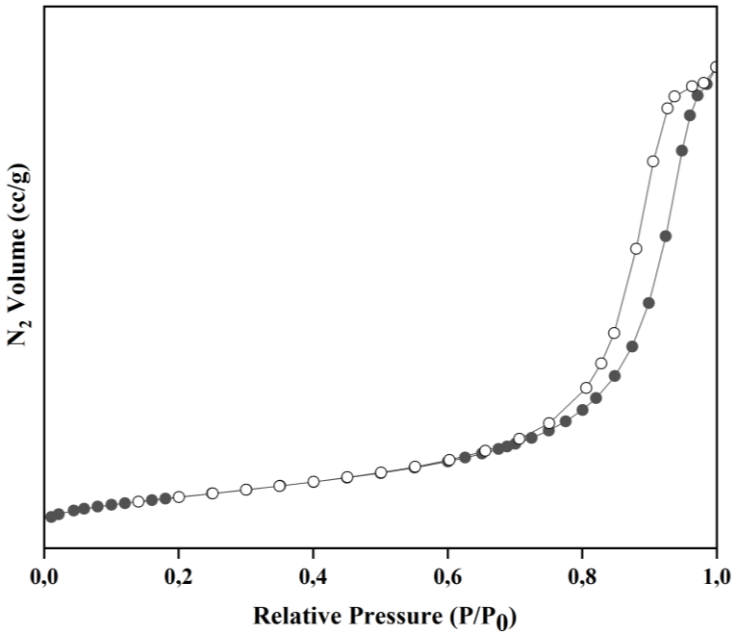

Fig. 4. Nitrogen adsorption desorption isotherm of LP

Table 1. The result of surface area mesurement

Catalyst	S_{BET} (m^2/g)	Pore Volume (cm^3/g)	Pore Diameter (nm)
LP	51.04	0.21	13.31

The nitrogen adsorption-desorption isotherm pattern from LP was shown in Fig. 4. Based on the IUPAC (International Union in Pure and Applied Chemistry) classification, all samples show type IV isothermal adsorption patterns which indicates the characteristic of mesoporous materials [23]. LP has H1 hysteresis which indicates the presence of specific narrow neck pores [14]. The result of surface area measurements are presented in Table 1. Pore size distribution analysis was carried out using the BJH method. The BJH method is used as a method to determine the pore size distribution of mesopores with a diameter of 2-50 nm [24]. The pore size distribution curve of LP is presented in Fig. 5. Peak at 18.77 nm was observed on the plot indicating the presence of pores in the mesoporous range, with an average pore size of 18.77 nm.

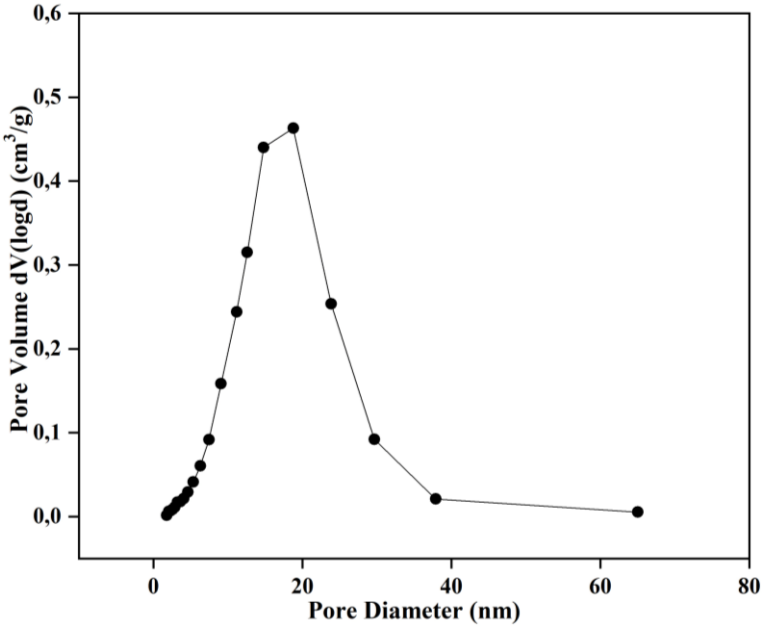

Fig. 5. BJH pore size distribution of LP

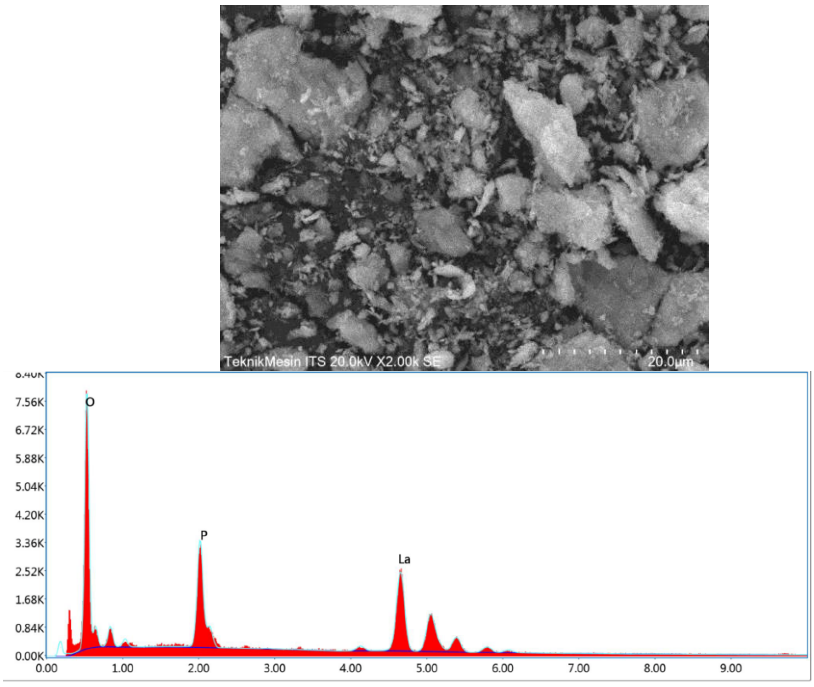

Fig. 6. SEM-EDX of LP

Fig. 6. show the SEM analysis morphology of LP. The morphology of LP is small particles that gather together to form aggregates and basically irregular in shape with an indefinite particle size. The composition of elements contained in LP was observed by SEM-EDX. The results of the EDX spectrum show that the obtained powder consists of La, P, and O. It indicates that no other elements were formed during the synthesis process.

3.1 Catalytic Test

The LP catalyst was tested for its activity in the conversion reaction of cellulose, glucose and fructose to 5-HMF. The 5-HMF formation was carried out using the hydrothermal method at high temperatures [25–27]. The filtrate obtained was then analyzed using UV-Vis spectrophotometer to determine the amount of product formed (5-HMF) and intermediate products (glucose and fructose). The presence of 5-HMF is indicated by a peak at ± 284 nm [26,28]. The conversion and yield of 5-HMF were shown in Fig. 7.

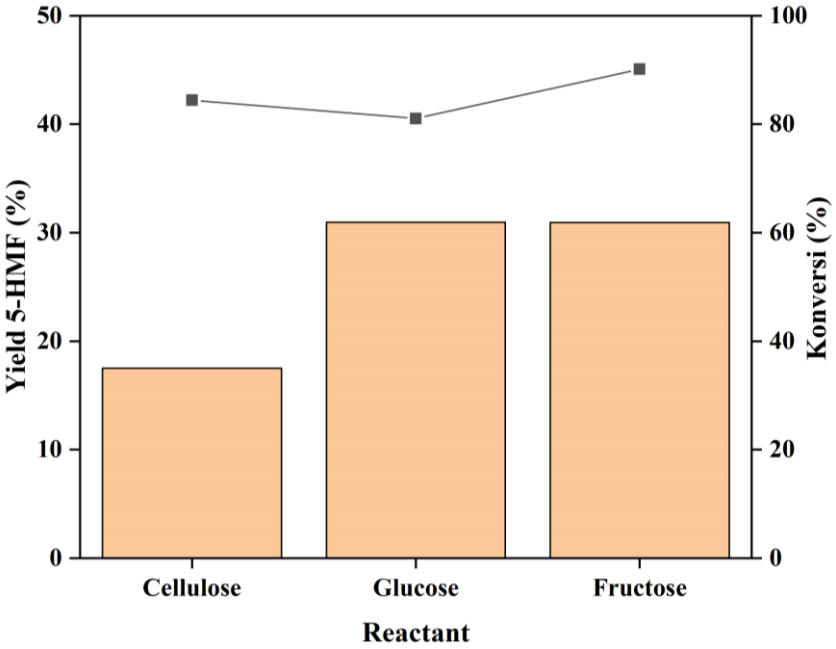

Fig. 7. Conversion and yield of 5-HMF by LP catalyst

The conversion reaction of cellulose to 5-HMF occurs in three main stages [29]. The first stage is the hydrolysis reaction from cellulose to glucose. This is then continued with the second stage, namely the isomerization reaction of glucose into fructose and the third stage, namely the dehydration of fructose into 5-HMF [30]. In Fig. 7, the conversion of glucose and fructose to 5-HMF is higher than the conversion of cellulose to 5-HMF. This is because the use of cellulose reactants requires 3 stages to form 5-HMF, while glucose and fructose require 2 and 1 stages respectively to form 5-HMF. The same thing also happened to the higher yield of 5-HMF produced from glucose and fructose reactants compared to cellulose reactants.

The correlation between catalysis results and characterization results was observed with the help of catalyst profiles and characterization. If the profile obtained is the same, then the catalyst character influences the catalysis parameters displayed. Through further observations, the profile of the conversion and yield of 5-HMF was linked to the results of

the characterization that had been carried out including acidity, crystallinity and surface area [31,32]. It has been found that the acidity of a catalyst is a key factor in its ability to convert cellulose reactants into products. Specifically, the formation of 5-HMF is highly dependent on the acidity of the catalyst, which ultimately affects its ability to convert the reactant into 5-HMF. The first and third stage reactions are influenced by Bronsted acids, while the second stage reactions are influenced by Lewis acids [33]. In Fig. 3, it can be seen that the Lewis acidity of the LP catalyst tends to be higher than the Bronsted acidity. This can be proven from the yield of 5-HMF with the glucose reactant which tends to be higher compared to the fructose reactant. Apart from that, the B/L acidity combination also has an important role in the yield of 5-HMF [32].

5 Conclusion

LP has been successfully synthesized using the sol-gel method at room temperature. XRD characterization revealed that the LP has hexagonal crystal structure. The S_{BET} surface area of Lanthanum phosphate is 51,04 m^2/g. SEM morphology observations indicate that the Lanthanum phosphate has an irregular shape with an indefinite particle size. EDX results indicate that La, P, and O elements are dispersed on the solid surface. Catalytic testing shows that the acidity of the catalyst has main role in the formation of 5-HMF.

Acknowledgement

This work was supported by the Ministry of Research, Technology, and Higher Education, Republic of Indonesia, under the research scheme of Penelitian Fundamental Riset (PFR) Grant in 2023.

References

1. V. Balaram, Geosci. Front. **10**, 1285 (2019)
2. M. J. Weber, a V Dotsenko, L. B. Glebov, and V. a Tsekhomsky, *Handbook of Phosphors* (2003)
3. R. R. Chada, S. S. Enumula, S. Reddy K, M. D. Gudimella, S. R. Rao Kamaraju, and D. R. Burri, Microporous Mesoporous Mater. **300**, 110144 (2020)
4. S. Sankar, B. N. Nair, T. Suzuki, G. M. Anilkumar, M. Padmanabhan, U. N. S. Hareesh, and K. G. Warrier, Sci. Rep. **6**, 4 (2016)
5. T. Gavrilović, J. Periša, J. Papan, K. Vuković, K. Smits, D. J. Jovanović, and M. D. Dramićanin, J. Lumin. **195**, 420 (2018)
6. Z. Wu, S. Yang, and W. Wu, Nanoscale **8**, 1237 (2016)
7. A. Kumar and R. Srivastava, (2020)
8. T. T. N. Nguyen, V. Ruaux, L. Massin, C. Lorentz, P. Afanasiev, F. Maugé, V. Bellière-Baca, P. Rey, and J. M. M. Millet, Appl. Catal. B Environ. **166**–**167**, 432 (2015)
9. D. Steinbach, A. Klier, A. Kruse, J. Sauer, S. Wild, and M. Zanker, Processes **7**, 1 (2020)
10. T. Zhang, H. Wei, H. Xiao, W. Li, Y. Jin, W. Wei, and S. Wu, Mol. Catal. **498**, 111254 (2020)
11. Y. Shao, Y. Ding, J. Dai, Y. Long, and Z. T. Hu, Green Synth. Catal. **2**, 187 (2021)

12. Y. Zhao, S. Wang, H. Lin, J. Chen, and H. Xu, RSC Adv. **8**, 7235 (2018)
13. I. F. Ulfindrayani, A. Zulys, F. Kurniawan, I. Nurfia, Q. A'yuni, M. Tamyiz, and I. K. Murwani, Rasayan J. Chem. **16**, 1864 (2023)
14. M. A. Ahmadzadeh, S. F. Chini, and A. Sadeghi, Mater. Des. **181**, 108058 (2019)
15. S. Y. Song, J. F. Ma, J. Yang, M. H. Cao, H. J. Zhang, H. S. Wang, and K. Y. Yang, Inorg. Chem. **45**, 1201 (2006)
16. W. B. Bu, Z. Le Hua, L. X. Zhang, H. R. Chen, W. M. Huang, and J. L. Shi, J. Mater. Res. **19**, 2807 (2004)
17. Z. Wang, J. G. Li, Q. Zhu, B. N. Kim, and X. Sun, Mater. Des. **126**, 115 (2017)
18. N. Niu, P. Yang, Y. Wang, W. Wang, F. He, S. Gai, and D. Wang, J. Alloys Compd. **509**, 3096 (2011)
19. K. A. Layman, M. M. Ivey, and J. C. Hemminger, J. Phys. Chem. B **107**, 8538 (2003)
20. H. Nur, Z. Ramli, J. Efendi, A. N. A. Rahman, S. Chandren, and L. S. Yuan, Catal. Commun. **12**, 822 (2011)
21. N. Rohmah, Q. A'yuni, and I. K. Murwani, in *AIP Conf. Proc. Vol. 2818. No. 1* (2023)
22. C. Cochon, T. Corre, S. Celerier, and S. Brunet, Appl. Catal. A Gen. **413**–**414**, 149 (2012)
23. Q. A'yuni, A. Rahmayanti, H. Hartati, P. Purkan, R. Subagyo, N. Rohmah, L. R. Itsnaini, and M. A. Fitri, RSC Adv. **13**, 2692 (2023)
24. H. Hartati, Q. A'yuni, N. H. Saputri, D. Z. Mardho, P. B. D. Firda, H. Hartono, H. Bahruji, R. E. Nugraha, N. A. Sholeha, and D. Prasetyoko, Catalysts **13**, 122 (2023)
25. Y. Shao, D. C. W. Tsang, D. Shen, Y. Zhou, Z. Jin, D. Zhou, W. Lu, and Y. Long, Environ. Res. **184**, 109340 (2020)
26. Y. F. Li, Y. P. Yuan, K. K. Wang, J. Jia, X. L. Qin, and Y. Xu, Iran. J. Chem. Chem. Eng. **32**, 75 (2013)
27. H. Xia, S. Xu, X. Yan, and S. Zuo, Fuel Process. Technol. **152**, 140 (2016)
28. Y. Yuan, S. Yao, S. Nie, and S. Wang, BioResources **11**, 2381 (2016)
29. X. Li, L. Zhang, S. Wang, and Y. Wu, **7**, 1 (2020)
30. J. S. M. Nogueira, V. T. Santana, P. V. Henrique, L. G. de Aguiar, J. P. A. Silva, S. I. Mussatto, and L. M. Carneiro, Catalysts **10**, 1 (2020)
31. X. Li, K. Peng, X. Liu, Q. Xia, and Y. Wang, ChemCatChem **9**, 2739 (2017)
32. K. Saravanan, K. S. Park, S. Jeon, and J. W. Bae, ACS Omega **3**, 808 (2018)
33. Q. S. Kong, X. L. Li, H. J. Xu, and Y. Fu, Fuel Process. Technol. **209**, 106528 (2020)